Method of sensitivity improving in the non-dispersive infrared gas analysis system

Youwen Sun (孙友文), Wenqing Liu (刘文清)*, Shimei Wang (汪世美), Shuhua Huang (黄书华), and Xiaoman Yu (于晓曼)

Key Laboratory of Environmental Optics and Technology, Anhui Institute of Optics and Fine Mechanics, Chinese Academy of Sciences, Hefei 230031, China

**Corresponding author: wqliu@aiofm.ac.cn*

Received November 9, 2010; accepted January 3, 2011; posted online April 28, 2011

A method of interference correction for improving the sensitivity of non-dispersive infrared (NDIR) gas analysis system is demonstrated. Based on the proposed method, the interference due to water vapor and carbon dioxide in the NDIR NO analyzer is corrected. After interference correction, the absorbance signal at the NO filter channel is only controlled by the absorption of NO, and the sensitivity of the analyzer is improved greatly. In the field experiment for pollution source emission monitoring, the concentration trend of NO monitored by NDIR analyzer is in good agreement with the differential optical absorption spectroscopy NO analyzer. Small variations of NO concentration can also be resolved, and the measuring correlation coefficient of the two analyzers is 94.28%.

OCIS codes: 010.0010, 010.1120.
doi: 10.3788/COL201109.060101.

Nitrogen oxides (NO + NO_2 or N_2O) are commonly emitted into the atmosphere from high-temperature combustion facilities during industrial production[1,2]. When nitrogen oxides and volatile organic compounds (VOCs) are exposed to sunlight in the atmosphere, they undergo various chemical reactions, producing secondary products that are involved in photochemical smog. Some of the products are harmful to human health, including ozone, poly aromatic hydrocarbons (PAH), peroxides, and peroxyacetic nitric anhydrides (PAN)[3].

Non-dispersive infrared (NDIR) gas analyzers are ideal equipments for a continuous emission monitoring system (CEMS). They typically have high measuring sensitivity. However, the sensitivity of these gas analyzers depends on the relative humidity of the operating environment and the concentration of interfering gases such as carbon dioxide (CO_2). Thus, a NDIR gas analyzer for measuring low concentrations of a target gas on the order of parts per million (ppm) should be effective in correcting such interference[4−7]. In this letter, we report on a method of correction for interfering water vapor and CO_2 to improve the sensitivity of a NDIR NO analyzer. It aims to investigate the feasibility of high-sensitivity measurement of NO in the pollutant source.

Figure 1 shows the functional layout of the NDIR NO analyzer, including a power source, an infrared (IR) optical source, an optical filter wheel, a filter controller, a sample cell, a detector assembly, and a data processor. During operation, the optical signal generated by the IR light source passes through the optical filter wheel and the sample cell, and finally arrives at the detector assembly. The filter controller selects different optical filters in sequence to modulate the optical signal using different frequency bands of optical energy. Based on the absorption of optical signal by the sample gas at different frequencies, the analyzer can account for the absorbance interference and detect which types of gases are present in the sample.

The IR optical source is a glowing metal filament heated to a temperature of 1200 K, which generates an optical signal in the IR spectrum with a broad range of optical wavelengths from 1.5 to 10 μm. The optical filter wheel includes four filters which can filter the optical wavelengths at a certain frequency band (the reference filter is used to produce reference signal to adjust for drift, such as the voltage drift on IR light source, external vibration, etc.). Figure 2 presents the IR absorption spectra of NO, H_2O, and CO_2. The parameters of all filters are clearly shown in Table 1. The sample cell includes three spherical mirrors to increase the optical path length of the modulated optical signal when it passes through the sample gas. The configuration of such a sample cell allows for 12-m optical path length within the 60-cm-long multi-pass cell. This results in more accurate determination of gas type, greater sensitivity, and more accurate gas concentration readings. The detector is a lead selenide device (SensArray Infrared, USA), which has good response performance between 1 and 10 μm.

There is a large concentration of humidity and CO_2 in many environments where NDIR NO analyzers are used. Both water vapor and CO_2 may have an IR absorption spectrum overlapping that of NO[8]. Figure 3 shows the absorption line intensity comparison among CO_2, H_2O, and NO at the NO filter channel on the y-axis and the wavelength on the x-axis. The location of the primary

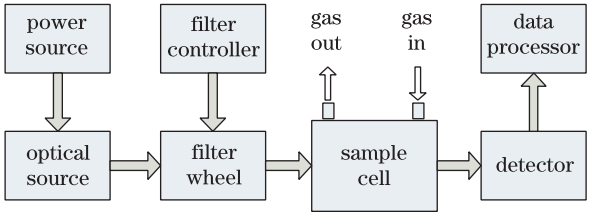

Fig. 1. Functional layout of NO gas analyzer.

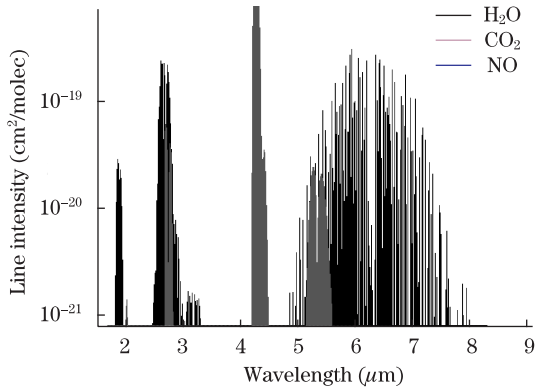

Fig. 2. IR absorption spectra of three molecules.

Table 1. Parameter Settings of Each Filter

	#1	#2	#3	#4
Filters	Ref	H_2O	NO	CO_2
Center Wavelength (μm)	3.73	2.59	5.25	4.3
Transmission (%)	76	94	80	93

absorption band of NO, shown between the two thick solid in Fig. 3, corresponds to some absorption by water vapor and CO_2. Therefore, without correction, filter #3 (which is designed to detect NO) would respond to CO_2, H_2O, and NO. Consequently, the sensitivity of the NDIR NO analyzer declines because of the two interfering gases[8−10].

To subtract the response due to water vapor from the output signal, the H_2O band pass filter must be designed to have a pass band with no absorption by NO. Moreover, to subtract the response due to CO_2 from the output signal, the CO_2 band bass filter must be designed to pass wavelengths associated with CO_2 absorption but not to transmit substantially at wavelengths associated with NO absorption. The two preferred filters are available in our analyzer.

The optical absorption of light due to the presence of the target gas in the sample cell is based on Lambert-Beer's law as

$$I(\lambda) = I_0(\lambda)\exp[-\alpha(\lambda)CL]. \quad (1)$$

When there are three absorbing species presented in the sample cell, Eq. (1) becomes

$$I(\lambda) = I_0(\lambda)\exp(-\alpha C_1 L) \cdot \exp(-\beta C_2 L)\cdot\exp(-\gamma C_3 L), \quad (2)$$

where $I_0(\lambda)$ is the optical intensity measured while sampling high-purity zero air; $I(\lambda)$ is the optical intensity measured while sampling the sample gas; α, β, and γ represent the absorption coefficients of three different gases; C_1, C_2, and C_3 represent the corresponding concentration of the three gases; L is the path length as a result of reflections in the sample cell. When the arguments of the exponentials are small, the following approximation of Eq. (2) can be used for the three gases[9,10]:

$$I(\lambda) = I_0(\lambda)(1 - \alpha C_1 L - \beta C_2 L - \gamma C_3 L). \quad (3)$$

When considering all the three filter channels (and a reference filter channel to adjust for drift) simultaneously, three equations can be established. Lambert-Beer's law from Eq. (3) can be written as

$$I^{\mathrm{N}}(\lambda) = I_0^{\mathrm{N}}(\lambda)(1 - \alpha_{\mathrm{N}}C_{\mathrm{N}}L - \beta_{\mathrm{N}}C_{\mathrm{H}}L - \gamma_{\mathrm{N}}C_{\mathrm{C}}L), \quad (4)$$

$$I^{\mathrm{H}}(\lambda) = I_0^{\mathrm{H}}(\lambda)(1 - \alpha_{\mathrm{H}}C_{\mathrm{N}}L - \beta_{\mathrm{H}}C_{\mathrm{H}}L - \gamma_{\mathrm{H}}C_{\mathrm{C}}L), \quad (5)$$

$$I^{\mathrm{C}}(\lambda) = I_0^{\mathrm{C}}(\lambda)(1 - \alpha_{\mathrm{C}}C_{\mathrm{N}}L - \beta_{\mathrm{C}}C_{\mathrm{H}}L - \gamma_{\mathrm{C}}C_{\mathrm{C}}L), \quad (6)$$

where NO is represented by N, water vapor by H, and CO_2 by C; α_{N}, α_{H}, and α_{C} represent the absorption coefficients of NO at NO, H_2O, and CO_2 filter channels, respectively; β_{N}, β_{H}, and β_{C} represent the absorption coefficients of H_2O at NO, H_2O, and CO_2 filter channels, respectively; C_{N}, C_{H}, and C_{C} represent the concentrations of NO, H_2O, and CO_2 presented in the sample cell, respectively.

The detector produces voltages that are proportional to the light-intensity signals received at each of the three filter channels. These voltages are given as

$$V^{\mathrm{N}} = V_0^{\mathrm{N}}(1 - \alpha_{\mathrm{N}}C_{\mathrm{N}}L - \beta_{\mathrm{N}}C_{\mathrm{H}}L - \gamma_{\mathrm{N}}C_{\mathrm{C}}L), \quad (7)$$

$$V^{\mathrm{H}} = V_0^{\mathrm{H}}(1 - \alpha_{\mathrm{H}}C_{\mathrm{N}}L - \beta_{\mathrm{H}}C_{\mathrm{H}}L - \gamma_{\mathrm{H}}C_{\mathrm{C}}L), \quad (8)$$

$$V^{\mathrm{C}} = V_0^{\mathrm{C}}(1 - \alpha_{\mathrm{C}}C_{\mathrm{N}}L - \beta_{\mathrm{C}}C_{\mathrm{H}}L - \gamma_{\mathrm{C}}C_{\mathrm{C}}L). \quad (9)$$

Equations (7–9) can be deduced as

$$A^{\mathrm{N}} = \frac{V^{\mathrm{N}}}{V_0^{\mathrm{N}}} = (1 - \alpha_{\mathrm{N}}C_{\mathrm{N}}L - \beta_{\mathrm{N}}C_{\mathrm{H}}L - \gamma_{\mathrm{N}}C_{\mathrm{C}}L), \quad (10)$$

$$A^{\mathrm{H}} = \frac{V^{\mathrm{H}}}{V_0^{\mathrm{H}}} = (1 - \alpha_{\mathrm{H}}C_{\mathrm{N}}L - \beta_{\mathrm{H}}C_{\mathrm{H}}L - \gamma_{\mathrm{H}}C_{\mathrm{C}}L), \quad (11)$$

$$A^{\mathrm{C}} = \frac{V^{\mathrm{C}}}{V_0^{\mathrm{C}}} = (1 - \alpha_{\mathrm{C}}C_{\mathrm{N}}L - \beta_{\mathrm{C}}C_{\mathrm{H}}L - \gamma_{\mathrm{C}}C_{\mathrm{C}}L), \quad (12)$$

where A^{N}, A^{H}, and A^{C} represent the total absorbances at NO, H_2O, and CO_2 filter channels, respectively. The absorption coefficients depend on the optical wavelengths selected using the appropriate band pass filters. In our analyzer, the filter characteristics are given such that the

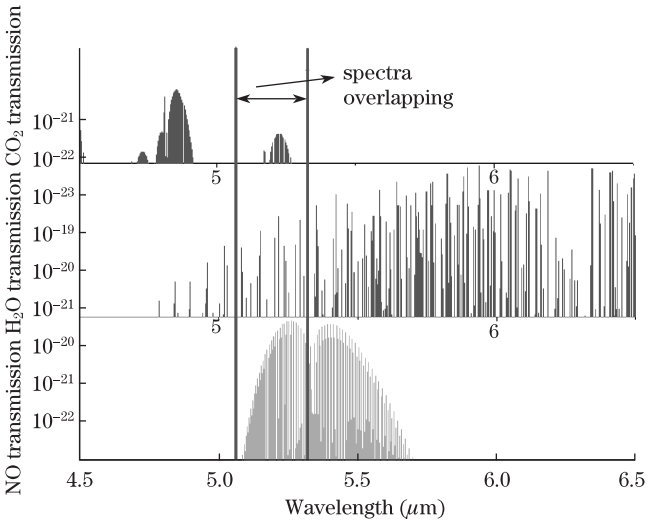

Fig. 3. Absorption spectra of H_2O, CO_2, and NO at the NO filter channel.

following relationships hold. (1) $\alpha_{\rm H} \cong \gamma_{\rm H} \cong 0$, H_2O channel has negligible response to NO and CO_2; (2) $\frac{\alpha_{\rm C}}{\gamma_{\rm C}} \cong \frac{\beta_{\rm C}}{\gamma_{\rm C}} \cong 0$, the water vapor and NO response sensitivities of the CO_2 band pass filter are negligible with respect to the CO_2 one, such that Eqs. (11) and (12) can be written as

$$A^{\rm H} = \frac{V^{\rm H}}{V_0^{\rm H}} = 1 - \beta_{\rm H} C_{\rm H} L, \tag{13}$$

$$A^{\rm C} = \frac{V^{\rm C}}{V_0^{\rm C}} = 1 - \gamma_{\rm C} C_{\rm C} L. \tag{14}$$

Based on Eqs. (13) and (14), Eq. (10) can be given as

$$\begin{aligned} A^{\rm N} &= \frac{V^{\rm N}}{V_0^{\rm N}} \\ &= \left(1 - \alpha_{\rm N} C_{\rm N} L - \frac{\beta_{\rm N}}{\beta_{\rm H}} \cdot \beta_{\rm H} C_{\rm H} L - \frac{\gamma_{\rm N}}{\gamma_{\rm C}} \cdot \gamma_{\rm C} C_{\rm C} L\right) \\ &= \left[1 - \alpha_{\rm N} C_{\rm N} L - \frac{\beta_{\rm N}}{\beta_{\rm H}}(1 - A^{\rm H}) - \frac{\gamma_{\rm N}}{\gamma_{\rm C}}(1 - A^{\rm C})\right]. \end{aligned} \tag{15}$$

In such a consequence, the pure absorbance of NO can be derived as

$$\begin{aligned} A_{\rm NO} &= \gamma_{\rm N} C_{\rm N} L \\ &= 1 - \frac{V^{\rm N}}{V_0^{\rm N}} - \frac{\beta_{\rm N}}{\beta_{\rm H}}\left(1 - \frac{V^{\rm H}}{V_0^{\rm H}}\right) - \frac{\gamma_{\rm N}}{\gamma_{\rm C}}\left(1 - \frac{V^{\rm C}}{V_0^{\rm C}}\right). \end{aligned} \tag{16}$$

Since $\gamma_{\rm N} L$ is constant, $A_{\rm NO}$ represents a signal that varies linearly to the NO concentration $C_{\rm N}$ in the presence of water vapor and CO_2. When the concentration of interfering water vapor and CO_2 changes, the corresponding $\frac{V^{\rm H}}{V_0^{\rm H}}$ and $\frac{V^{\rm C}}{V_0^{\rm C}}$ also changes, hence the interference can be corrected. Thus, the sensitivity of the absorbance signal $A_{\rm NO}$ is only controlled by the NO absorption at the NO filter channel. $\frac{\beta_{\rm N}}{\beta_{\rm H}}$ is defined as the response coefficient of H_2O at the NO filter channel, and $\frac{\gamma_{\rm N}}{\gamma_{\rm C}}$ is the response coefficient of CO_2 at the NO filter channel. Both parameters can be drawn from the HITRAN database. Interference due to water vapor and CO_2 is corrected on the basis of six voltages received by the detector. A similar method can also be used to improve the detection sensitivity of other NDIR gas analyzers.

As mentioned above, the response coefficients of H_2O and CO_2 at the NO filter channel are key factors for interference correction. Table 2 shows the response coefficients of NO, H_2O, and CO_2 at each filter channel acquired through line-by-line integration on the absorption line parameters provided by the HITRAN database, ignoring some infinite small coefficients[11,12]. The horizontal axis represents the filter channel and the vertical axis represents the type of gas. the response coefficient of H_2O at the NO filter channel is 0.04227, whereas that of CO_2 at the NO filter channel is 0.01106, i.e., in Eq. (16), $\frac{\beta_{\rm N}}{\beta_{\rm H}} = 0.04227$ and $\frac{\gamma_{\rm N}}{\gamma_{\rm C}} = 0.011106$.

Table 2. Response Coefficients of H_2O, NO, and CO_2 at Each Channel

	1 Ref	2 H_2O	3 NO	4 CO_2
H_2O	0	1	0.04227	0
NO	0	0	1	0
CO_2	0	0	0.011106	1

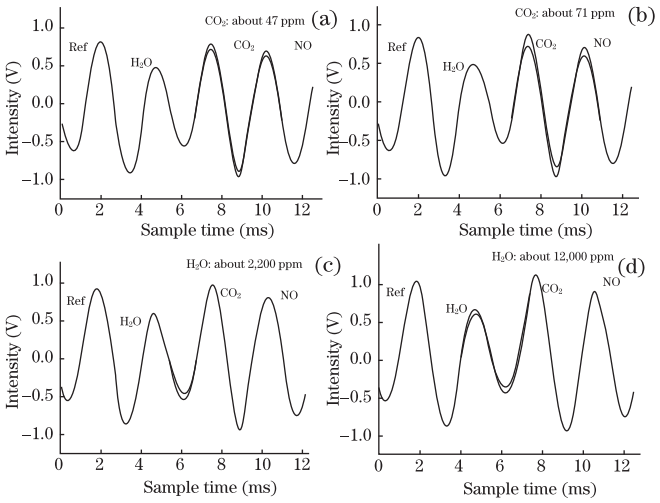

Fig. 4. Signal intensities at each channel before and after interference correction. Concentrations of CO_2 are about (a) 47 ppm and (b) 71 ppm; Concentrations of H_2O are (c) 2,200 ppm and (d) 12,000 ppm.

When the sample cell is filled with different concentrations of H_2O and CO_2, we use the response coefficients available from Table 2 to correct the interference with the method mentioned above. The signal intensities at each filter channel after correction are shown in Fig. 4 (only a portion of the results is included because of the large amount of data). The figure shows that after interference correction, signal intensity at the NO filter channel has no change or negligible change, except at the interfering gas filter channel, even if the concentrations of interfering gases are different, which proves that the method for interference correction is feasible.

Figure 5 is the calibration linearity of the analyzer after interference correction. The fitting correlation coefficient is shown to be 0.9999. The concentration of NO varies linearly to its absorbance calculated through Eq. (16) and $\gamma_{\rm N} L$ is constant. Thus, the absorbance can be regarded as a whole when is calibrated[13], which results in an easy and convenient calibration.

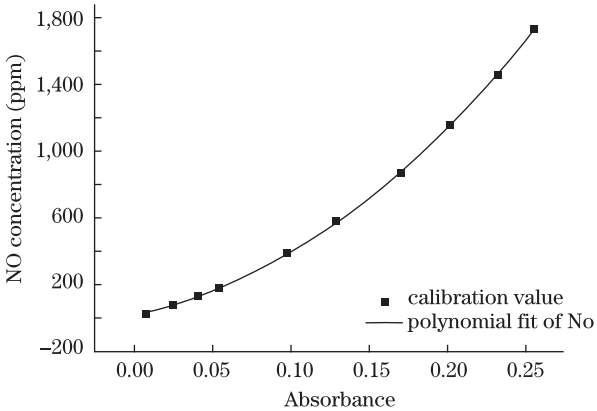

Fig. 5. Calibration linearity of the NDIR NO analyzer.

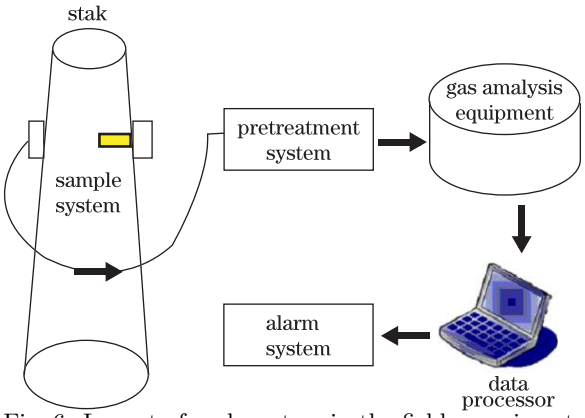

Fig. 6. Layout of each system in the field experiment.

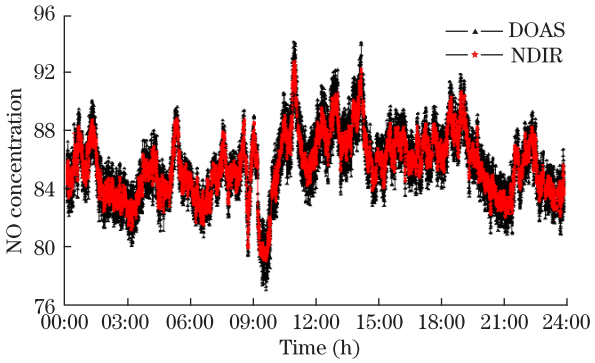

Fig. 7. Online monitoring comparison between the NDIR NO and DOAS NO analyzers.

We also made a field experiment in a steel company (Tong-Ling, Anhui Province, China). The NDIR analyzer and the differential potical absorption (DOAS) analyzer were installed parallelly to the roof of a building near the stack in order to monitor smoke pollution sampled from about 50 m above the ground. Figure 6 shows the layout of each system in the field experiment. The two analyzers were placed inside the gas analysis equipment. The sample gas was pretreated before connecting to the analyzer to cool high-temperature gas and remove particulates. Concentration readings monitored by the analyzers were automatically transmitted to the data processor on the ground. When the readings are abnormal, the alarm system will be triggered. The two analyzers were used for monitoring continuously for two days. Figure 7 presents the online monitoring comparison between the NDIR NO and DOAS NO analyzers in one day. It shows that the concentration trend of the two analyzers is almost the same during the monitoring time of 24 h, and that the emission concentration of NO from the stack is mainly concentrated in 82–92 ppm. Small variations of NO concentration can be resolved because of the high sensitivity of the NDIR NO analyzer after interference correction. Figure 8 shows the correlation graph of the two systems (data sampling for every 30 min), with the measuring correlation coefficient of the two analyzers at about 94.28%.

In conclusion, we present a correction method for interference due to H_2O and CO_2 in the NDIR gas analyzer. Based on the proposed method, the interference

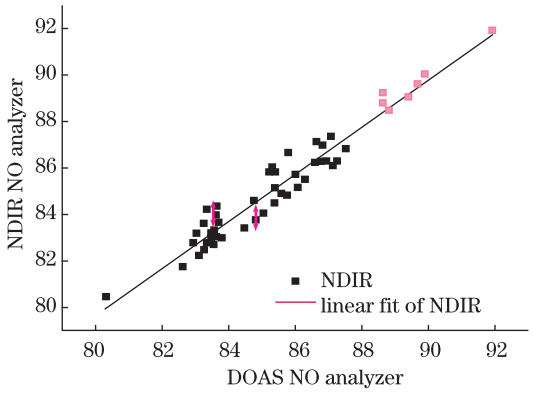

Fig. 8. Correlation of the NDIR NO and DOAS NO analyzers.

due to CO_2 and water vapor is corrected. The correlation coefficient of calibration after interference correction is up to 0.99991. In the field experiment for pollution source CO_2 emission monitoring, the trend of NO concentration monitored by the NDIR NO analyzer has a good agreement with that of the DOAS NO analyzer, and small variations of NO concentration can be resolved. The measuring correlation coefficient of the two analyzers is 94.28%. A similar method can also be used to improve the detection sensitivity of other NDIR gas analyzers.

This work was supported by the National "863" Project of China (No. 2009AA063006), the National Natural Science Foundation of China (No. 40805015), and the Excellent Youth Scientifie Foundation of Anhui (No. 10040606Y28).

References

1. A. J. de Castro, J. Meneses, S. Briz, and F. Lopez, Rev. Scient. Instrum. **70,** 3156 (1999).
2. W. Yan, Z. Tian, L. Pan, and M. Ding, Chin. Opt. Lett. **7,** 201 (2009).
3. H. C. Frey, N. M. Rouphail, A. Unal, and J. D. Colyar, in *Proceedings of Annual Meeting of Air* and *Waste Management Association 2001* (2001).
4. J. Y. Wong, "Simple multi-channel ndir gas", U.S. Patent US 7,329,870B2 (2008).
5. H. H. Asadov, I. M. Mirzabalayev, D. Z. Aliyev, J. A. Agayev, S. R. Azimova, N. A. Nabiyev, and S. N. Abdullayeva,S Chin. Opt. Lett. **7,** 361 (2009).
6. L. Ding, W. Liu, Y. Zhang, F. Si, M. Gao, F. Qi, and Y. Wang, Chin. J. Quantum **20,** 459 (2003).
7. X. Chen, J. Liu, F. Si, and W. Liu, Opto-Electron. Eng. **35,** 114 (2008).
8. H. Nakamura, "Vehicle-installed exhaust gas analyzing apparatus", U.S. Patent US 6,865,472B2 (2005).
9. L. Tyson, Y.-C. Ling, and C. K. Mann, App. Spectrosc. **38,** 663 (1984).
10. A. Galais, G. Fortunato, and P. Chavel, Appl. Opt. **24,** 2127 (1985).
11. J. Fang, W. Liu, and T. Zhang, Spectrosc. Spect. Anal. **28,** 1269 (2008).
12. H. Zhang and G. Shi, Chin. J. Atmos. Sci. **24**, 1 (2000).
13. A. Lehto, "Callbration method for gas concentration measurements", U.S. Patent 5369278 (2008).